



ORIGINAL ARTICLE

Uptake of positron emission tomography tracers reflects the tumor immune status in esophageal squamous cell carcinoma

Kengo Kuriyama¹  | Tamami Higuchi² | Takehiko Yokobori³ | Hideyuki Saito¹ | Tomonori Yoshida¹ | Keigo Hara¹ | Shigemasa Suzuki¹ | Makoto Sakai¹ | Makoto Sohda¹ | Tetsuya Higuchi⁴ | Yoshito Tsushima⁴ | Takayuki Asao² | Kyoichi Kaira⁵  | Hiroyuki Kuwano¹ | Ken Shirabe⁶ | Hiroshi Saeki¹

¹Division of Gastroenterological Surgery, Department of General Surgical Science, Gunma University Graduate School of Medicine, Maebashi, Japan

²Department of Oncology Clinical Development, Gunma University Graduate School of Medicine, Maebashi, Japan

³Division of Integrated Oncology Research, Gunma University Initiative for Advanced Research (GIAR), Maebashi, Japan

⁴Department of Diagnostic Radiology and Nuclear Medicine, Gunma University Graduate School of Medicine, Maebashi, Japan

⁵Department of Respiration Medicine, Saitama Medical University, International Medical Center, Hidaka, Japan

⁶Department of General Surgical Science, Gunma University Graduate School of Medicine, Maebashi, Japan

Correspondence

Takehiko Yokobori, Division of Integrated Oncology Research, Gunma University Initiative for Advanced Research (GIAR), 3-39-22 Showa-machi, Maebashi, Gunma 371-8511, Japan.
Email: bori45@gunma-u.ac.jp

Kengo Kuriyama, Department of General Surgical Science, Graduate School of Medicine, Gunma University, 3-39-22 Showa-machi, Maebashi, Gunma 371-8511, Japan.
Email: m1720018@gunma-u.ac.jp

Funding information

Ono Pharmaceutical Company; BristolMyers Company

Abstract

The relationship between the local immune status and cancer metabolism regarding ¹⁸F-FDG and ¹⁸F-FAMT uptake in esophageal squamous cell carcinoma (ESCC) remains unknown. The present study examined the correlations between tumor immune status, clinicopathological factors, and positron emission tomography (PET) tracer uptake in ESCC. Forty-one ESCC patients who underwent ¹⁸F-FDG PET and ¹⁸F-FAMT PET before surgery were enrolled in the study. Immunohistochemistry was conducted for programmed death 1 (PD-1), CD8, Ki-67, CD34, GLUT1 (¹⁸F-FDG transporter) and LAT1 (¹⁸F-FAMT transporter). ESCC specimens with high tumoral PD-L1 and high CD8-positive lymphocytes were considered to have "hot tumor immune status." High PD-L1 expression (53.7%) was significantly associated with tumor/lymphatic/venous invasion ($P = 0.028$, 0.032 and 0.018), stage ($P = 0.041$), CD8-positive lymphocytes ($P < 0.001$), GLUT1 ($P < 0.001$), LAT1 expression ($P = 0.006$), Ki-67 labelling index ($P = 0.009$) and CD34-positive vessel counts ($P < 0.001$). SUVmax of ¹⁸F-FDG was significantly higher in high PD-L1 cases than in low PD-L1 cases ($P = 0.009$). SUVmax of ¹⁸F-FAMT was significantly higher in high PD-L1 ($P < 0.001$), high CD8 ($P = 0.012$) and hot tumor groups ($P = 0.028$) than in other groups. High SUVmax of ¹⁸F-FAMT (≥ 4.15) was identified as the only predictor of hot tumor immune status. High PET tracer uptake was significantly associated with cancer aggressiveness and hot tumor immune status in ESCC. PET imaging may be an effective tool to predict tumor immune status in ESCC with respect to immune checkpoint inhibitor sensitivity.

KEYWORDS

CD8, esophageal cancer, FAMT-PET, FDG-PET, hot tumor, PD-L1

Kengo Kuriyama and Tamami Higuchi contributed equally to this work.

This is an open access article under the terms of the Creative Commons Attribution-NonCommercial License, which permits use, distribution and reproduction in any medium, provided the original work is properly cited and is not used for commercial purposes.

© 2020 The Authors. *Cancer Science* published by John Wiley & Sons Australia, Ltd on behalf of Japanese Cancer Association.

1 | INTRODUCTION

Esophageal carcinoma is the sixth most common cause of cancer-related death worldwide.¹ Esophageal squamous cell carcinoma (ESCC) is the most common histological subtype of esophageal cancer in many countries, including Japan.^{2,3} Although multimodality therapies for ESCC have shown progress, patient outcome remains poor, with 5-year overall survival rates ranging from 15% to 20%.^{4,5} Cisplatin in combination with fluorouracil as first-line therapy followed by docetaxel or paclitaxel as second-line therapy with or without radiation is commonly used as a standard chemotherapy for metastatic ESCC in Japan.⁶ However, no treatment strategy has been established for ESCC patients who are refractory or intolerant to these standard therapies.

Immune checkpoint inhibitors (ICI) have dramatically changed the treatment of melanoma, and their efficacy has also been reported in other cancers, including ESCC.⁷⁻⁹ Targeting of immune checkpoint proteins, such as programmed death 1 (PD-1), and its ligand-1 (PD-L1) results in a continuous and significant clinical effect with low toxicity in some responder patients.¹⁰⁻¹⁴ Since March 2020, nivolumab, as a representative ICI targeting PD-1, has been covered by the medical insurance system for ESCC in Japan. In contrast, almost all non-responder patients show no benefits on expensive ICI, accompanied by adverse immune-related events.¹⁵ Kato et al⁹ showed that the disease control rate for patients who received nivolumab treatment was 37%, and the fraction of non-responder patients was 55% in ESCC. Moreover, Stephane et al¹⁶ report that ICI may have a deleterious effect in a subset of patients by accelerating disease, referred to as “hyper-progressive disease.” Thus, useful biomarkers to estimate the sensitivity of patients to ICI are required in the clinic. Several recent studies have reported candidate biomarkers for estimating sensitivity to ICI, including tumor immune status (based on PD-L1-positive tumor cells and CD8 tumor infiltrating lymphocytes), tumor mutation burden, and interferon- γ (IFN- γ) gene signature.¹⁷⁻¹⁹ Tumor immune status with high PD-L1 expression/high numbers of infiltrating immune cells represents an ICI-sensitive “hot tumor,” whereas tumor immune status with low PD-L1 expression/poor infiltration of immune cells is considered a “cold tumor” and is associated with poor local immune response and ICI resistance.^{20,21} Non-invasive diagnostic methods that can distinguish hot and cold tumor statuses based on PD-L1 expression/infiltrating immune cells remain to be established.

Glucose and amino acid metabolism in tumor cells play crucial roles in the regulation of local anti-tumor immunity.²² The 2-deoxy-2-[fluorine-18] fluoro-D-glucose with positron emission tomography (¹⁸F-FDG PET) imaging modality based on glucose metabolism has been widely used for diagnosing malignant lesions.²³ Overexpression of glucose transporter 1 (GLUT1) is reported to be significantly correlated with ¹⁸F-FDG uptake in human cancers.²⁴ Recent studies have shown that PD-L1 expression in tumor cells is closely correlated with the uptake of ¹⁸F-FDG and GLUT1 expression in patients with non-small-cell lung cancer.^{25,26} Heiden

et al²⁷ used genome-wide expression analyses and demonstrated that esophageal adenocarcinoma tumors with high FDG uptake are significantly associated with PD-L1 expression. Another study showed that L-[3-¹⁸F]- α -methyltyrosine (¹⁸F-FAMT) PET, which is based on amino acid metabolism and is associated with the L-type amino acid transporter 1 (LAT1), is useful in the detection of various neoplasms.²⁸ Previously, we reported the usability of ¹⁸F-FAMT PET in the diagnosis of ESCC.^{29,30} However, the relationship between the tumor immune status and cancer metabolism in ESCC remains unknown.

The present study aimed to clarify the association between local anti-tumor immunity and glucose and amino acid metabolism in ESCC. Therefore, we examined ¹⁸F-FDG and ¹⁸F-FAMT uptake in PET imaging and the expression levels of PD-L1, CD8, GLUT1 and LAT1 in ESCC tissue samples using immunohistochemistry to determine whether non-invasive PET imaging results can be used as a predictive biomarker for tumor immune status to identify cases with probable ICI sensitivity.

2 | MATERIALS AND METHODS

2.1 | Patients

A total of 41 patients with pathologically confirmed ESCC who underwent surgical resection from April 2008 to December 2011 at Gunma University Hospital were included in this study. Samples and medical records of the same patients included in the previous study³⁰ were used. All patients received a pre-treatment work-up with imaging studies including ¹⁸F-FDG PET and ¹⁸F-FAMT PET. None of the patients received chemotherapy or radiotherapy preoperatively or had any concomitant malignancy or heart disease. Staging was based on the 7th edition of the TNM classification system of the Union for International Cancer Control. The follow-up duration for censored cases ranged from 3.8 to 129 months (median: 60.6 months). This study conformed to the tenets of the Helsinki Declaration and was approved by the Institutional Review Board for Clinical Research at the Gunma University Hospital (Maebashi, Gunma, Japan; approval number: HS2019-213). Patient agreement was obtained with the opt-out method.

2.2 | Immunohistochemistry

Four-micron sections were cut from paraffin blocks of all 41 samples. Each section was mounted on a silane-coated glass slide, deparaffinized in xylene, rehydrated, and incubated for 30 minutes at room temperature in 0.3% hydrogen peroxide to block endogenous peroxidases. After rehydration through a graded series of ethanol treatments, antigen retrieval was performed in Immunosaver (Nisshin EM) at 98-100°C for 45 minutes. Nonspecific binding sites were blocked by incubating with Protein Block Serum-Free (Dako) for 30 minutes at room temperature. Samples were incubated

overnight at 4°C with the following primary antibodies overnight: PD-L1 (E1L3N Rabbit mAb, 1:100 dilution, Cell Signaling), CD8 (ab4055, 1:1500 dilution, Abcam), GLUT1 (ab15309, 1:200 dilution, Abcam), LAT1 (4A2, 1:3200 dilution, J-Pharma), Ki-67 (1:40 dilution, Dako) and CD34 (1:800 dilution, Nichirei). A Histofine Simple Stain MAX-PO (Multi) Kit (Nichirei) was used as the secondary antibody. We applied chromogen 3,3-diaminobenzidine tetrahydrochloride as a 0.02% solution in 50 mmol/L ammonium acetate-citrate acid buffer (pH 6.0) containing 0.005% H₂O₂. The sections were lightly counterstained with hematoxylin and mounted.

Programmed death ligand-1 expression was evaluated as positive when membrane staining was observed. A semi-quantitative scoring method was used for PD-L1 based on a previous study: 1 ≤ 1%, 2 = 1%-5%, 3 = 6%-10%, 4 = 11%-25%, 5 = 26%-50% and 6 ≥ 50% of positive cells.²⁵ Tumors with a score ≥ 3 were graded as high PD-L1 expression. CD8 was semi-quantitatively evaluated based on the extent of positive lymphocytes infiltrating the ESCC specimens; we defined patients with more than 5% positive lymphocytes as positive for CD8. Although definite cut-off value rates of PD-L1 and CD8 expression that indicated hot tumor immune status were not defined, we designated patients with more than 5% positive tumor cells of PD-L1 and more than 5% CD8 positive tumor infiltrating lymphocytes as having hot tumor immune status in this study. For GLUT1 and LAT1, a semi-quantitative scoring method was used as follows: 1 ≤ 10%, 2 = 11%-25%, 3 = 26%-50%, 4 = 51%-75% and 5 ≥ 76% of tumor area stained. Tumors with scores of 4 or 5 were defined as high expression. For Ki-67, we examined a highly cellular area of the immunostained sections. Epithelial cells with nuclear staining of any intensity were defined as high expression. We counted approximately 1000 nuclei on each slide. Proliferative activity was assessed as the percentage of Ki-67-stained nuclei (Ki-67 labelling index) in the sample. The median value of the Ki-67 labelling index was 41% (range, 10%-80%). The number of CD34-positive vessels was counted in four selected hotspots in a 400× field (0.26 mm² field area). CD34-positive vessel counts were defined as the mean microvessel counts per 0.26 mm² field area. These evaluation methods are based on previous studies.^{30,31}

The tissue sections were examined under a light microscope by two independent investigators who were blinded to the patient data. In case of discrepancies, both investigators examined the slides simultaneously until a final consensus on the assessment was obtained.

2.3 | Positron emission tomography imaging and data analysis

We synthesized ¹⁸F-FAMT in our cyclotron facility according to a previously described method.²⁸ The radiochemical yield of ¹⁸F-FAMT was approximately 20%, and the radiochemical purity was approximately 99%. We also produced ¹⁸F-FDG in

our facility as described previously.³² The patients fasted for at least 6 hours before PET imaging. One of two PET/CT scanners (Discovery STE, GE Healthcare; Biograph 16, SIEMENS Healthcare) was randomly selected with a 700-mm field of view. Three-dimensional data acquisition was initiated 50 minutes after the injection of 5 MBq/kg of ¹⁸F-FAMT or 5 MBq/kg of ¹⁸F-FDG. We acquired 4-10 bed positions (3 minutes acquisition per bed position) according to the range of imaging. Attenuation-corrected transverse images obtained with ¹⁸F-FAMT and ¹⁸F-FDG were reconstructed using the ordered-subset expectation maximization algorithm into 128 × 128 matrices with a slice thickness of 3.27 mm. All ¹⁸F-FAMT and ¹⁸F-FDG PET images were evaluated by two experienced nuclear physicians. Tracer uptake in the primary tumor was defined as a positive finding if the uptake was higher than that in the normal mediastinum. Any discrepant results were resolved by consensual review. For semiquantitative analysis, functional images of the standardized uptake value (SUV) were produced based on the attenuation-corrected transaxial images, the injected doses of ¹⁸F-FAMT and ¹⁸F-FDG (MBq), the patients' body weight (g), and the cross-calibration factor between PET and the dose calibrator. The SUV (MBq/g) of the lesion was defined as the radioactive concentration in the region of interest (ROI) divided by the injected dose (MBq) and the patient's body weight (g). The ROI was manually drawn over the primary tumor on the SUV images. When the tumor was >1 cm in diameter or if the shape of the tumor was irregular or multifocal, a ROI of approximately 1 cm in diameter was drawn over the area corresponding to the maximal tracer uptake. ROI analysis was performed by a nuclear physician with the aid of the corresponding CT scans. The maximal SUV in the ROI (SUVmax) was used as a representative uptake value for evaluating the ¹⁸F-FAMT and ¹⁸F-FDG uptake in the primary lesion for statistical analyses.

2.4 | Statistical analysis

Statistical analyses were performed with the Mann-Whitney *U* test for continuous variables and the χ^2 -test for categorical variables. The correlation between SUVmax for ¹⁸F-FAMT and ¹⁸F-FDG on PET and different variables was analyzed using Spearman's correlation coefficient tests. Kaplan-Meier curves were used for overall survival, and statistical significance was determined using the log-rank test. Univariate analysis was performed with each predictive factor using logistic regression analysis for a hot tumor immune status, defined as high PD-L1 and high CD8-positive lymphocytes in ESCC tissues. Receiver operating characteristic (ROC) curve analyses were used to evaluate the potential of SUVmax for ¹⁸F-FAMT and ¹⁸F-FDG to discriminate between hot tumor immune status and others. Sensitivity and specificity were calculated to detect the optimal cut-off value for the SUVmax using ROC curves. A probability value of <0.05 was considered significant. All statistical analyses were performed using JMP software (SAS Institute).

3 | RESULTS

3.1 | Immunohistochemical staining for programmed death ligand-1 and CD8 in clinical esophageal squamous cell carcinoma samples

In total, 41 patients with ESCC were enrolled in this study. PD-L1 immunostaining was detected in cancer cells and localized predominantly on the plasma membrane. PD-L1 expression levels in cancer tissues were higher than those in normal tissues (Figure 1A). CD8-positive lymphocytes were observed more frequently around cancer tissues than around normal tissues (Figure 1B). Representative images of ^{18}F -FDG PET and ^{18}F -FAMT PET in the same case of Figure 1A,B are shown in Figure 1C,D. The rates of high PD-L1 and CD8 expression were 53.7% (22/41) and 34.1% (14/41), respectively. Approximately 31.7% (13/41) of samples in this cohort showed hot tumor immune status. High levels of GLUT1 and LAT1 were identified in 68.3% (28/41) and 43.9% (18/41) of cases, respectively. The median Ki-67 labelling index was 41% (range, 10%-80%). The median number of CD34-positive vessels was 18 (range 5-35).

3.2 | Clinicopathological significance of programmed death ligand-1, CD8 and tumor immune status in esophageal squamous cell carcinoma

The correlations between clinicopathological characteristics of ESCC patients and PD-L1, CD8 and hot tumor immune status are described in Table 1. High PD-L1 expression was significantly associated with tumor invasion ($P = 0.028$), lymphatic invasion ($P = 0.032$), venous invasion ($P = 0.018$), stage ($P = 0.041$), CD8 expression ($P < 0.001$), GLUT1 expression ($P < 0.001$), LAT1 expression ($P = 0.006$), Ki-67 labelling index ($P = 0.009$) and CD34-positive vessel count ($P < 0.001$). High CD8 expression was correlated with high PD-L1 expression

($P < 0.001$) and a high Ki-67 labelling index ($P = 0.005$). Hot tumor immune status (with high PD-L1 and high CD8) was significantly associated with high GLUT1 expression ($P = 0.024$) and a high Ki-67 labelling index ($P = 0.014$).

Figure 2 presents the prognostic analyses of ESCC patients according to PD-L1 expression (Figure 2A), CD8 expression (Figure 2B) and hot tumor immune status (Figure 2C). ESCC patient groups with high PD-L1, high CD8 or hot tumor immune status were not associated with poor prognosis compared to the other groups.

3.3 | Relationship between ^{18}F -FDG/ ^{18}F -FAMT uptake and immune status of esophageal squamous cell carcinoma

Figure 3 shows the relationship between PET tracer uptake and immune status of ESCC. The SUVmax of ^{18}F -FDG in the high PD-L1 group was significantly higher than that in the low PD-L1 group ($P = 0.009$) (Figure 3A). CD8 expression and hot tumor immune status showed a tendency to be related with high SUVmax of ^{18}F -FDG ($P = 0.063$ and $P = 0.057$, respectively) (Figure 3A). The SUVmax values of ^{18}F -FAMT in the high PD-L1, high CD8 and hot tumor groups were significantly higher than those in the other groups ($P < 0.001$, $P = 0.012$ and $P = 0.028$, respectively) (Figure 3B).

3.4 | Diagnostic value of ^{18}F -FAMT uptake in predicting the hot tumor immune status in esophageal squamous cell carcinoma

We next analyzed the diagnostic value of clinicopathological factors and PET imaging to estimate the hot tumor immune status in the ESCC cohort. ROC analysis for the SUVmax of ^{18}F -FDG revealed that the optimal cut-off value for a hot tumor was 8.79 (area under

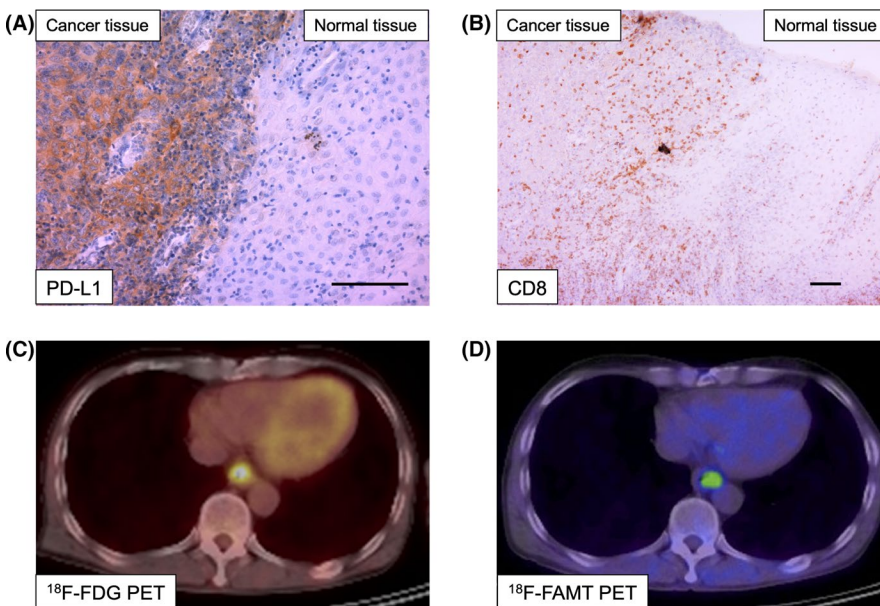


FIGURE 1 Representative immunohistochemical staining and positron emission tomography (PET) imaging of patients with esophageal squamous cell carcinoma (ESCC). Representative immunostaining for programmed death ligand-1 (PD-L1) (A, original magnification 200 \times) and CD8 (B, original magnification 100 \times) expression in slides containing both ESCC and normal tissue (scale bar = 100 μm). PET imaging of ^{18}F -FDG (C) and ^{18}F -FAMT (D) in the same patient is shown

TABLE 1 Association of clinicopathological features and programmed death ligand-1 (PD-L1) expression, CD8 expression, and hot tumor immune status in 41 esophageal squamous cell carcinoma (ESCC) patients

Factor	PD-L1 expression			CD8 expression			Tumor immune status		
	Low (n = 19)	High (n = 22)	P value	Low (n = 27)	High (n = 14)	P value	Hot tumor (high PD-L1/ high CD8, n = 13)	Others (n = 28)	P value
Age (y)									
Mean ± SD	67.7 ± 7.1	65.6 ± 6.3	.32	67.0 ± 6.8	65.9 ± 6.7	.64	65.4 ± 6.6	67.2 ± 6.7	.43
Sex									
Male	15	21	.11	23	13	.48	12	24	.55
Female	4	1		4	1		1	4	
Tumor invasion									
T1, T2	15	10	.028	17	8	.717	7	18	.524
T3, T4	4	12		10	6		6	10	
N factor									
Absent	9	5	.097	9	5	.879	4	10	.756
Present	10	17		18	9		9	18	
Lymphatic invasion									
Absent	7	2	.032	6	3	.954	2	7	.489
Present	12	20		21	11		11	21	
Venous invasion									
Absent	9	3	.018	9	3	.427	3	9	.553
Present	10	19		18	11		10	19	
Stage									
Stage I, II	13	8	.041	15	6	.441	5	16	.266
Stage III, IV	6	14		12	8		8	12	
PD-L1 expression									
Low	-	-	-	18	1	<.001	-	-	-
High	-	-		9	13		-	-	
CD8 positive lymphocytes									
Low	18	9	<.001	-	-	-	-	-	-
High	1	13		-	-		-	-	
GLUT1									
Low	11	2	<.001	11	2	.084	1	12	.024
High	8	20		16	12		12	16	
LAT1									
Low	15	8	.006	16	7	.571	6	17	.382
High	4	14		11	7		7	11	
Ki-67 labeling index									
Mean ± SD	36.8 ± 19.2	52.4 ± 17.6	.009	39.1 ± 18.2	56.7 ± 17.8	.005	56.1 ± 18.3	40.1 ± 18.6	.014
CD34 positive vessels counts									
Mean ± SD	13.9 ± 5.3	22.1 ± 5.9	<.001	17.0 ± 7.0	21.0 ± 6.0	.075	20.9 ± 6.2	17.1 ± 7.0	.103

the curve [AUC], 0.654; $P = 0.05$, sensitivity, 69.2%, specificity, 60.7%; Figure 4A), and ROC analysis for the SUVmax of ^{18}F -FAMT showed a cut-off value of 4.15 (AUC, 0.701; $P = 0.025$, sensitivity, 38.5%, specificity, 92.9%; Figure 4B). The ESCC patients were divided into high and low groups according to these cut-off points. The high SUVmax of ^{18}F -FAMT by non-invasive ^{18}F -FAMT-PET was the

only predictive factor for the hot tumor immune status (OR, 0.12; 95% CI, 0.02-0.69; $P = 0.02$; Table 2). The other clinicopathological factors were not significantly associated with hot tumor immune status. Using the cut-off value of 4.15 for the SUVmax of ^{18}F -FAMT, the accuracy rate of ^{18}F -FAMT-PET that predicts hot tumor immune status was 75.6%, and the positive predictive value was 71.4%.

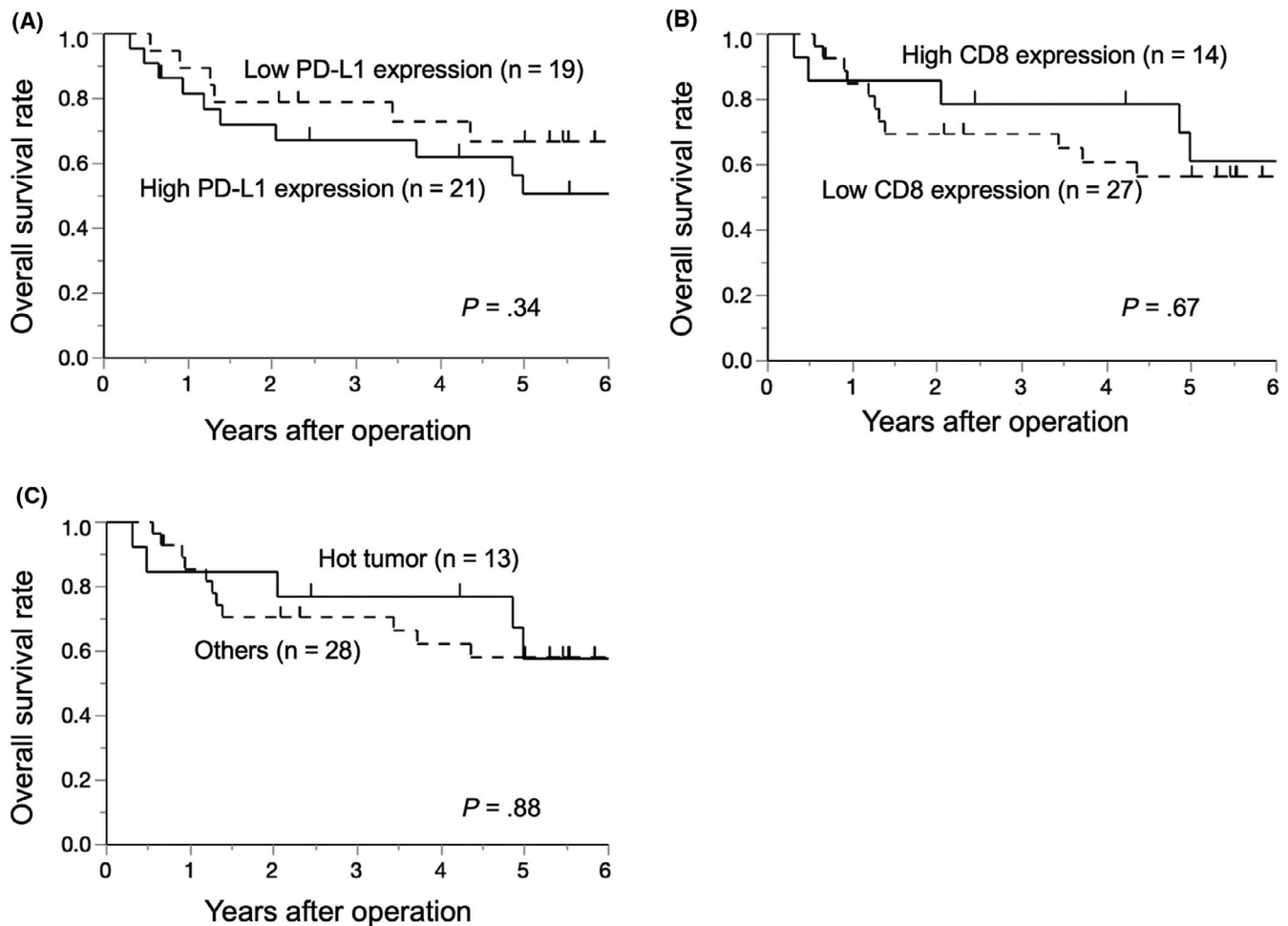


FIGURE 2 Overall survival of the study population according to programmed death ligand-1 (PD-L1) expression, CD8 expression and hot tumor immune status. A, Overall survival of esophageal squamous cell carcinoma (ESCC) patients according to tumoral PD-L1 expression. B, Overall survival of ESCC patients according to infiltrating CD8-positive lymphocytes. C, Overall survival of ESCC patients according to hot tumor immune status defined as high tumoral PD-L1 expression and high infiltrating CD8-positive lymphocytes in ESCC tissues. ESCC patient groups with high PD-L1, high CD8 or hot tumor immune status were not associated with poor prognosis compared to the other groups

4 | DISCUSSION

In this study, we demonstrated that high expression levels of PD-L1 in ESCC were significantly associated with the progression of tumor invasion, lymphatic invasion, venous invasion, stage, CD8-positive lymphocytes, GLUT1 expression, LAT1 expression, Ki-67 labelling index, and CD34-positive vessel count. In addition, we showed that the SUVmax of ^{18}F -FDG was significantly correlated with PD-L1 expression, and the SUVmax of ^{18}F -FAMT was significantly associated with high PD-L1, high CD8 expression, and hot tumor immune status. The high SUVmax of ^{18}F -FAMT was the only predictor of the hot tumor phenotype.

The efficacy of ICI is affected by PD-L1 expression of the tumor, as well as by the local anti-tumor immunity of cancer patients. Tumors with a higher density of infiltrating immune cells, called hot tumors, are more responsive to ICI than cold tumors with a lower density of infiltrating immune cells.^{20,21} In ESCC, the usability of PD-L1 expression as a biomarker of ICI sensitivity remains

controversial.^{9,33} However, in other cancers, several studies have reported the predictive value of ICI sensitivity markers, such as tumoral PD-L1 expression,³⁴ hot tumor phenotype,^{20,21} tumor mutation burden³⁵ and IFN- γ gene signature.^{36,37} In our study, we examined the expression of not only PD-L1 but also CD8-positive lymphocyte infiltration in ESCC to indicate hot tumor immune status and demonstrated a positive correlation between PET-imaging results and hot tumor phenotype in ESCC. These data suggested that PET-imaging as a predictor of PD-L1 and CD8 expression may be associated with ICI sensitivity in ESCC. However, we could not estimate a direct association between ICI sensitivity, local anti-tumor immunity, and PET imaging in our cohort without ICI treatment. Further studies are thus required to evaluate the clinical significance of PET imaging as an ICI sensitivity marker in ESCC patients who have received ICI therapy.

In ESCC recurrence cases, especially in mediastinal or abdominal lymph node recurrence, obtaining tumor samples is difficult. As mentioned above, PD-L1 expression, hot tumor phenotype, tumor

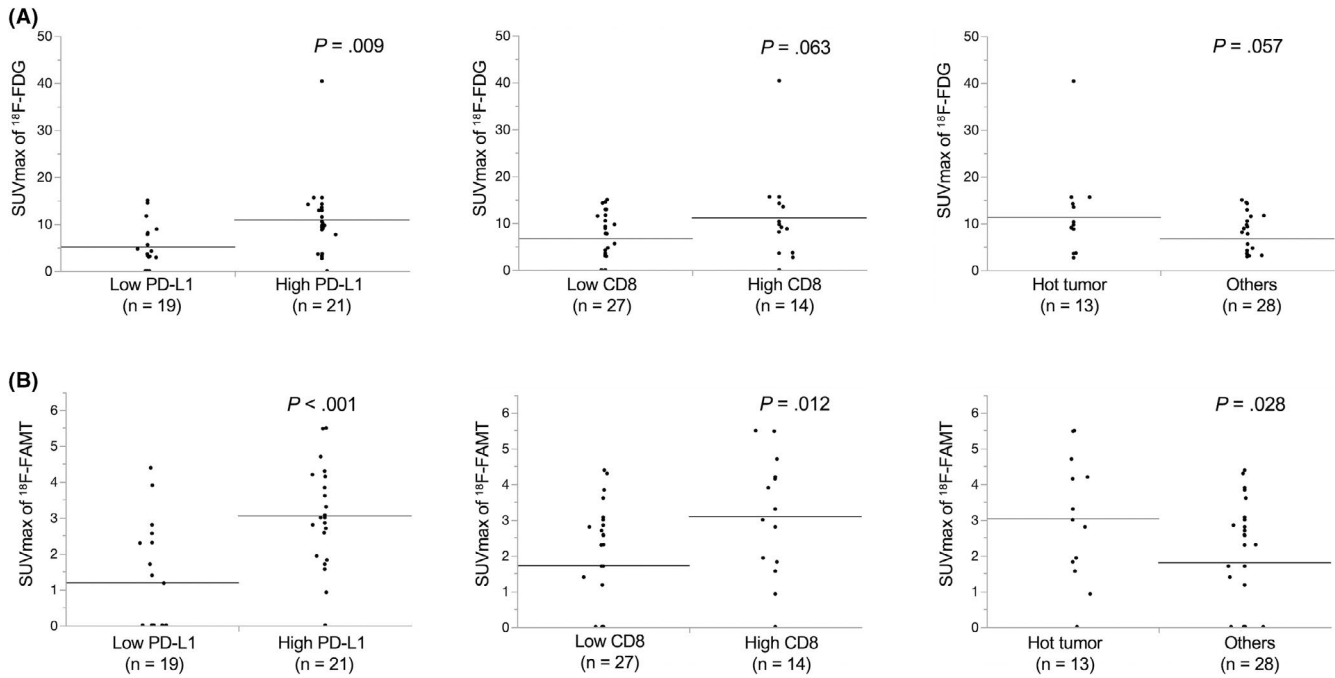
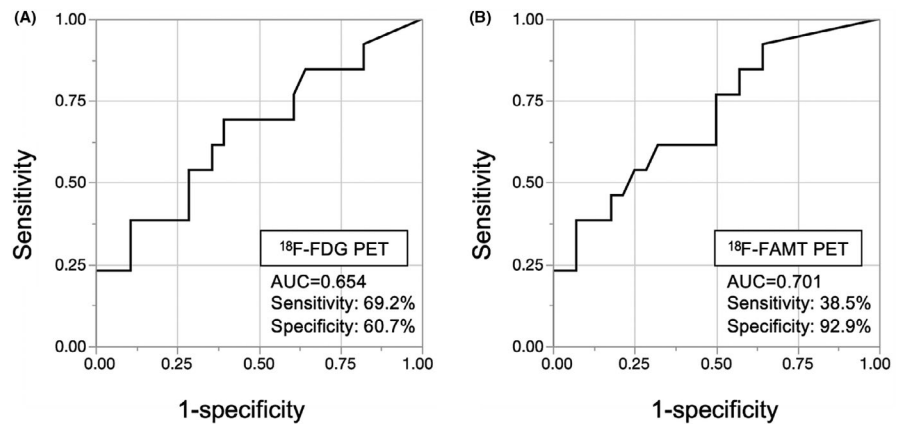


FIGURE 3 Relationship between positron emission tomography (PET) tracer uptake and programmed death ligand-1 (PD-L1), CD8 and hot tumor immune status in esophageal squamous cell carcinoma tissues. A, Correlation between SUVmax of ^{18}F -FDG and PD-L1, CD8 and hot tumor immune status. SUVmax of ^{18}F -FDG in high PD-L1 cases was significantly higher than that in low PD-L1 cases ($P = 0.009$). B, Correlation between SUVmax of ^{18}F -FAMT and PD-L1, CD8 and hot tumor immune status. The SUVmax of ^{18}F -FAMT in the high PD-L1, high CD8 and hot tumor groups was significantly higher than that in the other groups ($P < 0.001$, $P = 0.012$ and $P = 0.028$, respectively)

FIGURE 4 Receiver operating characteristic (ROC) curve analyses for the optimal cut-off value of positron emission tomography (PET) tracer uptake. ROC analyses for the potential of SUVmax for ^{18}F -FDG (A) and ^{18}F -FAMT (B) to discriminate between hot tumor immune status and others. The areas under the curve for hot tumor immune status were 0.654 and 0.701 for SUVmax of ^{18}F -FDG and ^{18}F -FAMT, respectively



mutation burden and an IFN- γ gene signature were related to ICI sensitivity in several cancers. However, invasive procedures may be needed to obtain sufficient tumor tissues to evaluate these factors in patients with profound recurrent tumors in the thoracic or abdominal cavity. Although local immune status may be easily evaluable in primary tumors resected before recurrence, the primary tumor and metastatic/recurrent lesions may show differences in phenotype and tumor immune status. The heterogeneity of PD-L1 status between the primary cancer lesion and metastatic lymph nodes has been reported in triple negative breast cancer, clear cell renal cancer and bladder cancer.³⁸⁻⁴⁰ In addition, the tumor tissue obtained from the previous surgical treatment for the primary site may be considered old in comparison with that obtained from the

current profound recurrent lymph node. Therefore, real-time monitoring of immune status in metastatic/recurrent tumors is difficult using the existing techniques. Moreover, patients with advanced ESCC often show poor performance status because of poor oral intake, low nutrient condition, and cachexia; invasive procedures in such patients may cause severe adverse events. In our study, we showed that high uptake of ^{18}F -FDG and ^{18}F -FAMT by non-invasive PET imaging was significantly associated with a hot tumor phenotype, which has been associated with good response to ICI treatment in several cancers. These results suggest that non-invasive PET imaging can help evaluate the real-time expression of PD-L1 and CD8 in target lesions, independent of problems caused by temporal and spatial heterogeneity between the primary site

TABLE 2 Univariate analysis of factors associated with hot tumor immune status

Clinicopathologic variable	Univariate analysis		P value
	OR	95% CI	
Age ($\leq 65 / > 65$ y)	1.35	0.36-5.19	.66
Sex (male/female)	2	0.26-41.4	.53
T factor (T1, T2/T3, T4)	0.65	0.17-2.51	.53
N factor (absent/present)	0.8	0.18-3.18	.76
Lymphatic invasion (absent/present)	0.55	0.07-2.74	.48
Venous invasion (absent/present)	0.63	0.12-2.7	.55
SUVmax of ^{18}F -FDG (low/high)	0.29	0.06-1.11	.07
SUVmax of ^{18}F -FAMT (low/high)	0.12	0.02-0.69	.02

CI, confidence interval; OR, odds ratio.

and metastatic/recurrent lesions. This suggests the possibility of selecting ESCC patients who can receive the benefits of ICI without invasive tumor sampling.

Glucose and amino acid metabolism in tumor cells play crucial roles in the regulation of PD-L1 expression, which is important for anti-tumor immunity.²² GLUT1 and LAT1 are widely expressed in various human cancers,⁴¹⁻⁴⁶ and PET tracers such as ^{18}F -FDG and ^{18}F -FAMT are imported to tumor cells via GLUT1 and LAT1, respectively.^{24,47-49} High expression of LAT1 in cancer tissues can activate HIF-1 α /GLUT1 signaling through activation of mammalian target of rapamycin (mTOR).⁵⁰⁻⁵² Interestingly, Noman et al report that HIF-1 α directly binds to the hypoxia-responsive element in the proximal promoter of PD-L1 and can upregulate PD-L1 expression.⁵³ In our study, we demonstrated that PD-L1 expression in ESCC tissues was significantly correlated with the expression of GLUT1 and LAT1 (Table 1 and Figure S1). Moreover, our previous study showed that ^{18}F -FDG and ^{18}F -FAMT uptake in PET imaging is significantly associated with the expression levels of transporters for glucose and amino acids, such as GLUT1 and LAT1.³⁰ These results suggest that PET imaging for visualizing glucose and amino acid metabolism might reflect the expression levels of PD-L1 in local ESCC tissues through activation of the LAT1/HIF1 α /GLUT1/PD-L1 axis.

In our study, there was a statistically significant association between high PD-L1 expression and Ki-67 labeling index or CD34 positive vessel counts: activating receptor tyrosine kinase (RTK) or HIF1 α induced PD-L1.^{54,55} RTK activation upregulates the proliferative capacity of tumor cells, while HIF1 α plays a crucial role in angiogenesis by mediating vascular endothelial growth factor.⁵² Several studies have reported that the expression of PD-L1 is significantly correlated with proliferation ability and angiogenesis in cancer cells.⁵⁶⁻⁵⁸ Our study suggested that high PD-L1 ESCC patients had upregulated proliferation capacity and angiogenesis through RTK or HIF1 α activation.

Our study also shows the association between ^{18}F -FAMT uptake and CD8 positive lymphocyte infiltration, which constitutes

the indispensable element of hot tumors. LAT1 transports abundant neutral amino acids, such as tyrosine, leucine and tryptophan, into the cell.⁵⁹ Tryptophan is an essential amino acid that is metabolized through the kynurenine pathway, which is mainly catalyzed by indoleamine 2,3-dioxygenase.⁶⁰ Tryptophan deprivation causes immunosuppression due to the increased demand for tryptophan during T cell activation.²² However, the relationship between ^{18}F -FAMT-PET, LAT1 and tryptophan metabolism in ESCC has many ambiguities. Therefore, further studies are needed to clarify whether high uptake of ^{18}F -FAMT that depends on LAT1 can predict CD8 infiltration through tryptophan metabolism.

This study had several limitations. First, this was a retrospective single institution study, and we only enrolled patients without ICI treatment, such as nivolumab or pembrolizumab, and those who had undergone surgical resection, creating an unavoidable bias. Second, the number of patients in the study was small. Third, we did not perform any functional experiments on the associations among tumor PD-L1 expression, CD8-positive lymphocytes, and uptake of ^{18}F -FDG and ^{18}F -FAMT using in vitro and in vivo analyses.

In conclusion, we demonstrated that high uptake of PET tracers, such as ^{18}F -FDG and ^{18}F -FAMT, was correlated with PD-L1 and CD8 expression in ESCC. In addition, high level of ^{18}F -FAMT uptake was the only predictor of hot tumor immune status in ESCC, as indicated by high PD-L1 expression and increased CD8-positive lymphocytes. These observations suggest that PET imaging may be a good diagnostic tool to predict tumor immune status in ESCC cases associated with ICI sensitivity. Nonetheless, further studies are warranted to clarify the direct relationship between PET imaging and ICI treatment.

ACKNOWLEDGMENTS

We thank Ms Mariko Nakamura, Ms Yukie Saito, Ms Sayaka Okada, Ms Kayoko Takahashi, Ms Mizuho Murata, Ms Kanna Nakamura, Ms Harumi Kanai, Ms Fumie Takada and Ms Sawa Nagayama for their excellent assistance. We would like to thank Editage for English language editing. This work was supported in part by research grants from Ono Pharmaceutical Company and BristolMyers Company to KK

DISCLOSURE

Kengo Kuriyama, Takehiko Yokobori, Hideyuki Saito, Tomonori Yoshida, Keigo hara, Shigemasa Suzuki, Makoto Sakai, Makoto Sohda, Tetsuya Higuchi, Yoshito Tsushima, Takayuki Asao, Hiroyuki Kuwano, Ken Shirabe and Hiroshi Saeki have no conflicts of interest to declare. Tamami Higuchi is an employee of Fujifilm. Kyoichi Kaira has received research grants and is a speaker honorarium from Ono Pharmaceutical Company and BristolMyers.

ORCID

Kengo Kuriyama  <https://orcid.org/0000-0001-7365-0686>

Kyoichi Kaira  <https://orcid.org/0000-0001-5548-7686>

REFERENCES

1. Ferlay J, Soerjomataram I, Dikshit R, et al. Cancer incidence and mortality worldwide: sources, methods and major patterns in GLOBOCAN 2012. *Int J Cancer*. 2015;136:E359-E386.
2. Bray F, Ferlay J, Soerjomataram I, Siegel RL, Torre LA, Jemal A. Global cancer statistics 2018: GLOBOCAN estimates of incidence and mortality worldwide for 36 cancers in 185 countries. *CA Cancer J Clin*. 2018;68:394-424.
3. Abnet CC, Arnold M, Wei WQ. Epidemiology of oesophageal squamous cell carcinoma. *Gastroenterology*. 2018;154:360-373.
4. Rustgi AK, El-Serag HB. Oesophageal carcinoma. *N Engl J Med*. 2014;371:2499-2509.
5. Siegel RL, Miller KD, Jemal A. Cancer statistics, 2017. *CA Cancer J Clin*. 2017;67:7-30.
6. Kuwano H, Nishimura Y, Oyama T, et al. Guidelines for diagnosis and treatment of carcinoma of the esophagus april 2012 edited by the Japan oesophageal society. *Esophagus*. 2015;12:1-30.
7. Kudo T, Hamamoto Y, Kato K, et al. Nivolumab treatment for oesophageal squamous-cell carcinoma: an open-label, multicentre, phase 2 trial. *Lancet Oncol*. 2017;18:631-639.
8. Hodi FS, O'Day SJ, McDermott DF, et al. Improved survival with ipilimumab in patients with metastatic melanoma. *N Engl J Med*. 2010;363:711-723.
9. Kato K, Cho BC, Takahashi M, et al. Nivolumab versus chemotherapy in patients with advanced oesophageal squamous cell carcinoma refractory or intolerant to previous chemotherapy (ATTRACTION-3): a multicentre, randomised, open-label, phase 3 trial. *Lancet Oncol*. 2019;20:1506-1517.
10. Eggermont AMM, Blank CU, Mandala M, et al. Adjuvant pembrolizumab versus placebo in resected stage III melanoma. *N Engl J Med*. 2018;378:1789-1801.
11. Robert C, Schachter J, Long GV, et al. Pembrolizumab versus ipilimumab in advanced melanoma. *N Engl J Med*. 2015;372:2521-2532.
12. Gandhi L, Rodriguez-Abreu D, Gadgeel S, et al. Pembrolizumab plus chemotherapy in metastatic non-small-cell lung cancer. *N Engl J Med*. 2018;378:2078-2092.
13. Paz-Ares L, Luft A, Vicente D, et al. Pembrolizumab plus chemotherapy for squamous non-small-cell lung cancer. *N Engl J Med*. 2018;379:2040-2051.
14. Ferris RL, Blumenschein G, Fayette J, et al. Nivolumab for recurrent squamous-cell carcinoma of the head and neck. *N Engl J Med*. 2016;375:1856-1867.
15. Shields BD, Mahmoud F, Taylor EM, et al. Indicators of responsiveness to immune checkpoint inhibitors. *Sci Rep*. 2017;7:807.
16. Champiat S, Derclé L, Ammari S, et al. Hyperprogressive disease is a new pattern of progression in cancer patients treated by anti-PD-1/PD-L1. *Clin Cancer Res*. 2017;23:1920-1928.
17. Kim MY, Koh J, Kim S, Go H, Jeon YK, Chung DH. Clinicopathological analysis of PD-L1 and PD-L2 expression in pulmonary squamous cell carcinoma: comparison with tumor-infiltrating T cells and the status of oncogenic drivers. *Lung Cancer*. 2015;88:24-33.
18. De Meulenaere A, Vermassen T, Creytsens D, et al. Importance of choice of materials and methods in PD-L1 and TIL assessment in oropharyngeal squamous cell carcinoma. *Histopathology*. 2018;73:500-509.
19. Rizvi H, Sanchez-Vega F, La K, et al. Molecular determinants of response to anti-programmed cell death (PD)-1 and anti-programmed death-ligand 1 (PD-L1) blockade in patients with non-small-cell lung cancer profiled with targeted next-generation sequencing. *J Clin Oncol*. 2018;36:633-641.
20. Wargo JA, Reddy SM, Reuben A, Sharma P. Monitoring immune responses in the tumour microenvironment. *Curr Opin Immunol*. 2016;41:23-31.
21. Gujar S, Pol JG, Kroemer G. Heating it up: oncolytic viruses make tumours 'hot' and suitable for checkpoint blockade immunotherapies. *Oncoimmunology*. 2018;7:e1442169.
22. Gottfried E, Kreutz M, Mackensen A. Tumor metabolism as modulator of immune response and tumour progression. *Semin Cancer Biol*. 2012;22:335-341.
23. Vansteenkiste JF, Stroobants SG, Dupont PJ, et al. Prognostic importance of the standardized uptake value on (18)F-fluoro-2-deoxyglucose-positron emission tomography scan in non-small-cell lung cancer: an analysis of 125 cases. Leuven Lung Cancer Group. *J Clin Oncol*. 1999;17:3201-3206.
24. Kaira K, Endo M, Abe M, et al. Biologic correlation of 2-[18F]-fluoro-2-deoxy-D-glucose uptake on positron emission tomography in thymic epithelial tumours. *J Clin Oncol*. 2010;28:3746-3753.
25. Kasahara N, Kaira K, Bao P, et al. Correlation of tumour-related immunity with 18F-FDG-PET in pulmonary squamous-cell carcinoma. *Lung Cancer*. 2018;119:71-77.
26. Kaira K, Shimizu K, Kitahara S, et al. 2-Deoxy-2-[fluorine-18] fluoro-D-glucose uptake on positron emission tomography is associated with programmed death ligand-1 expression in patients with pulmonary adenocarcinoma. *Eur J Cancer*. 2018;101:181-190.
27. Heiden BT, Patel N, Nancarrow DJ, et al. Positron emission tomography 18F-fluorodeoxyglucose uptake correlates with KRAS and EMT gene signatures in operable oesophageal adenocarcinoma. *J Surg Res*. 2018;232:621-628.
28. Tomiyoshi K, Amed K, Muhammad S, et al. Synthesis of isomers of 18F-labelled amino acid radiopharmaceutical: position 2- and 3-L-18F-alpha-methyltyrosine using a separation and purification system. *Nucl Med Commun*. 1997;18:169-175.
29. Sohda M, Kato H, Suzuki S, et al. 18F-FAMT-PET is useful for the diagnosis of lymph node metastasis in operable oesophageal squamous cell carcinoma. *Ann Surg Oncol*. 2010;17:3181-3186.
30. Suzuki S, Kaira K, Ohshima Y, et al. Biological significance of fluorine-18-alpha-methyltyrosine (FAMT) uptake on PET in patients with oesophageal cancer. *Br J Cancer*. 2014;110:1985-1991.
31. Honjo H, Toh Y, Sohda M, et al. Clinical significance and phenotype of MTA1 expression in oesophageal squamous cell carcinoma. *Anticancer Res*. 2017;37:4147-4155.
32. Oriuchi N, Tomiyoshi K, Inoue T, et al. Independent thallium-201 accumulation and fluorine-18-fluorodeoxyglucose metabolism in glioma. *J Nucl Med*. 1996;37:457-462.
33. Shah MA, Kojima T, Hochhauser D, et al. Efficacy and safety of pembrolizumab for heavily pretreated patients with advanced, metastatic adenocarcinoma or squamous cell carcinoma of the esophagus: the Phase 2 KEYNOTE-180 Study. *JAMA Oncol*. 2019;5:546-550.
34. Garon EB, Rizvi NA, Hui R, et al. Pembrolizumab for the treatment of non-small-cell lung cancer. *N Engl J Med*. 2015;372:2018-2028.
35. Hellmann MD, Ciuleanu TE, Pluzanski A, et al. Nivolumab plus ipilimumab in lung cancer with a high tumour mutational burden. *N Engl J Med*. 2018;378:2093-2104.
36. Fehrenbacher L, Spira A, Ballinger M, et al. Atezolizumab versus docetaxel for patients with previously treated non-small-cell lung cancer (POPLAR): a multicentre, open-label, phase 2 randomised controlled trial. *Lancet*. 2016;387:1837-1846.
37. Ayers M, Luceford J, Nebozhyn M, et al. IFN-gamma-related mRNA profile predicts clinical response to PD-1 blockade. *J Clin Invest*. 2017;127:2930-2940.
38. Li M, Li A, Zhou S, et al. Heterogeneity of PD-L1 expression in primary tumours and paired lymph node metastases of triple negative breast cancer. *BMC Cancer*. 2018;18:4.
39. Jilaveanu LB, Shuch B, Zito CR, et al. PD-L1 expression in clear cell renal cell carcinoma: an analysis of nephrectomy and sites of metastases. *J Cancer*. 2014;5:166-172.

40. Mukherji D, Jabbour MN, Saroufim M, et al. Programmed death-ligand 1 expression in muscle-invasive bladder cancer cystectomy specimens and lymph node metastasis: a reliable treatment selection biomarker? *Clin Genitourin Cancer*. 2016;14:183-187.
41. Mueckler M, Thorens B. The SLC2 (GLUT) family of membrane transporters. *Mol Aspects Med*. 2013;34:121-138.
42. Blayney JK, Cairns L, Li G, et al. Glucose transporter 1 expression as a marker of prognosis in oesophageal adenocarcinoma. *Oncotarget*. 2018;9:18518-18528.
43. Kanai Y, Segawa H, Miyamoto K, Uchino H, Takeda E, Endou H. Expression cloning and characterization of a transporter for large neutral amino acids activated by the heavy chain of 4F2 antigen (CD98). *J Biol Chem*. 1998;273:23629-23632.
44. Nakanishi K, Ogata S, Matsuo H, et al. Expression of LAT1 predicts risk of progression of transitional cell carcinoma of the upper urinary tract. *Virchows Arch*. 2007;451:681-690.
45. Nawashiro H, Otani N, Shinomiya N, et al. L-type amino acid transporter 1 as a potential molecular target in human astrocytic tumours. *Int J Cancer*. 2006;119:484-492.
46. Ichinoe M, Mikami T, Yoshida T, et al. High expression of L-type amino-acid transporter 1 (LAT1) in gastric carcinomas: comparison with non-cancerous lesions. *Pathol Int*. 2011;61:281-289.
47. Kaira K, Serizawa M, Koh Y, et al. Relationship between 18F-FDG uptake on positron emission tomography and molecular biology in malignant pleural mesothelioma. *Eur J Cancer*. 2012;48:1244-1254.
48. Wiriyasermkul P, Nagamori S, Tominaga H, et al. Transport of 3-fluoro-L-alpha-methyl-tyrosine by tumour-upregulated L-type amino acid transporter 1: a cause of the tumour uptake in PET. *J Nucl Med*. 2012;53:1253-1261.
49. Kaira K, Oriuchi N, Otani Y, et al. Fluorine-18-alpha-methyltyrosine positron emission tomography for diagnosis and staging of lung cancer: a clinicopathologic study. *Clin Cancer Res*. 2007;13:6369-6378.
50. Fuchs BC, Bode BP. Amino acid transporters ASCT2 and LAT1 in cancer: partners in crime? *Semin Cancer Biol*. 2005;15:254-266.
51. Düvel K, Yecies JL, Menon S, et al. Activation of a metabolic gene regulatory network downstream of mTOR complex 1. *Mol Cell*. 2010;39:171-183.
52. Koh MY, Powis G. Passing the baton: the HIF switch. *Trends Biochem Sci*. 2012;37:364-372.
53. Noman MZ, Desantis G, Janji B, et al. PD-L1 is a novel direct target of HIF-1alpha, and its blockade under hypoxia enhanced MDSC-mediated T cell activation. *J Exp Med*. 2014;211:781-790.
54. Chen J, Jiang CC, Jin L, Zhang XD. Regulation of PD-L1: a novel role of pro-survival signalling in cancer. *Ann Oncol*. 2016;27:409-416.
55. Ji M, Liu Y, Li Q, et al. PD-1/PD-L1 pathway in non-small-cell lung cancer and its relation with EGFR mutation. *J Transl Med*. 2015;13:5.
56. Takada K, Okamoto T, Toyokawa G, et al. The expression of PD-L1 protein as a prognostic factor in lung squamous cell carcinoma. *Lung Cancer*. 2017;104:7-15.
57. Koh YW, Lee SJ, Han JH, Haam S, Jung J, Lee HW. PD-L1 protein expression in non-small-cell lung cancer and its relationship with the hypoxia-related signaling pathways: a study based on immunohistochemistry and RNA sequencing data. *Lung Cancer*. 2019;129:41-47.
58. Xue S, Hu M, Li P, et al. Relationship between expression of PD-L1 and tumor angiogenesis, proliferation, and invasion in glioma. *Oncotarget*. 2017;8:49702-49712.
59. Wang Q, Holst J. L-type amino acid transport and cancer: targeting the mTORC1 pathway to inhibit neoplasia. *Am J Cancer Res*. 2015;5:1281-1294.
60. Vécsei L, Szalárdy L, Fülöp F, Toldi J. Kynurenines in the CNS: recent advances and new questions. *Nat Rev Drug Discov*. 2013;12:64-82.

SUPPORTING INFORMATION

Additional supporting information may be found online in the Supporting Information section.

How to cite this article: Kuriyama K, Higuchi T, Yokobori T, et al. Uptake of positron emission tomography tracers reflects the tumor immune status in esophageal squamous cell carcinoma. *Cancer Sci*. 2020;111:1969-1978. <https://doi.org/10.1111/cas.14421>